Tunable Microstructures in Entropy-Stabilized Oxide Thin Films Studied with Unsupervised Machine Learning Assisted Electron Microscopy

Leixin Miao, George N Kotsonis, Jon-Paul Maria, Nasim Alem

2594
doi:10.1017/S1431927622009862
Microsc. Microanal. 28 (Suppl 1), 2022

Tunable Microstructures in Entropy-Stabilized Oxide Thin Films Studied with Unsupervised Machine Learning Assisted Electron Microscopy

Leixin Miao[1], George N. Kotsonis[1], Jon-Paul Maria[1] and Nasim Alem[1]

[1.] Department of Materials Science and Engineering, The Pennsylvania State University, University Park, PA, USA

A steady stream of new and advanced materials is crucial for scientific discovery and technology opportunities. High-entropy materials have become a rich new source of crystalline materials at the frontier of materials discovery. High entropy (HE) materials leverage increased configurational entropy to lower the overall free energy, stabilizing multiple atomic species into a single lattice.[1] HE materials have demonstrated promising functional properties for electrochemical[2], thermoelectric[3], catalytic[4], and many more applications. Entropy stabilization was first realized in high entropy alloys (HEAs). This concept was only recently expanded into the non-metallic crystals with the synthesis of the rocksalt structure high entropy oxides (R-HEOs) in 2015.[1,5] HEOs show inherent metastability at room temperature. Our previous studies on the HEO thin film synthesized with pulsed laser deposition (PLD) method demonstrated the metastability of the crystal at room temperature can be exploited for tuning the cation oxidation states with growth temperature.[6,7]

In this study, we further investigated the correlation between microstructure and the synthesis conditions in PLD grown R-HEO thin film with the composition $(Co_{0.2}Cu_{0.2}Mg_{0.2}Ni_{0.2}Zn_{0.2})O$ with advanced transmission electron microscopy (TEM) assisted by unsupervised machine learning. In particular, we focused on the impact of the growth rate and the film thickness on the microstructures. The samples for the study consisted of four epitaxial HEO thin films deposited at 400°C, with the laser pulse rate and the total thickness of 1) 5Hz & 80 nm, 2) 5Hz and 400 nm, 3) 1Hz and 80 nm, and 4) 1Hz and 400 nm.

The different synthesis conditions allow the crystal to reach various configurations and form distinct microstructures. For example, the thickness impacts the microstructure in the HEO thin films. Figure 1a shows the low angle annular dark field (LAADF) STEM image on the 5Hz & 400nm HEO thin film. Numerous cubic-shaped nanoscale microstructures with the spinel structure are embedded in the rock salt structured matrix and are highlighted by the strain contrast (bright). Figure 1b shows the atomic resolution STEM image of the atomic arrangement in the microstructure with the spinel structure.

On the other hand, a slower growth rate leads to a different configuration. Figure 2a shows the LAADF-STEM image of the 1Hz & 80 nm HEO thin film with the platelet microstructure forming on the {110} family of planes (called tweed). The unsupervised machine learning algorithm extracted the local distortion for the lattices within the tweed structures in Figure 2b and indicated a tetragonal distortion with a rotation of ±3 degrees. The energy-dispersive X-ray spectroscopy (EDX) elemental mapping shows an enriched Cu concentration at the tweed in Figure 2c. The EDX mapping indicates a potential correlation between the tetragonal distortion and the Jahn-Teller distortion for Cu ions. This study successfully demonstrates kinetic phase engineering in the HEO thin films [8].

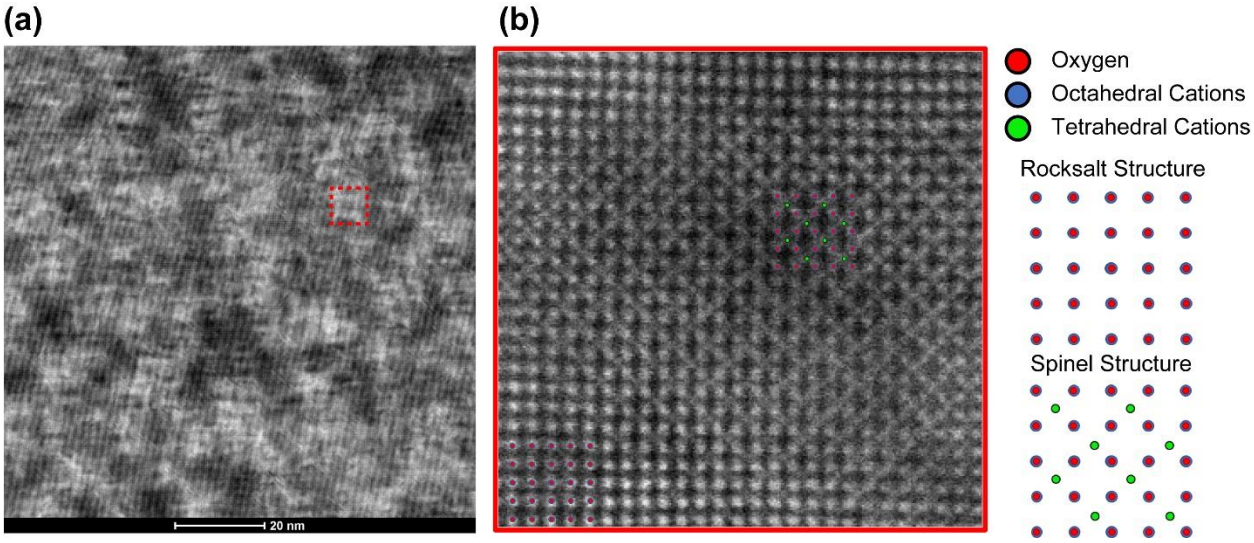

Figure 1. (a) the low angle annular dark field (LAADF) STEM image on the 5Hz & 400nm HEO thin film showing the cuboid-shaped microstructures. (b) the atomic resolution STEM image of the atomic arrangement in the microstructure with the spinel structure.

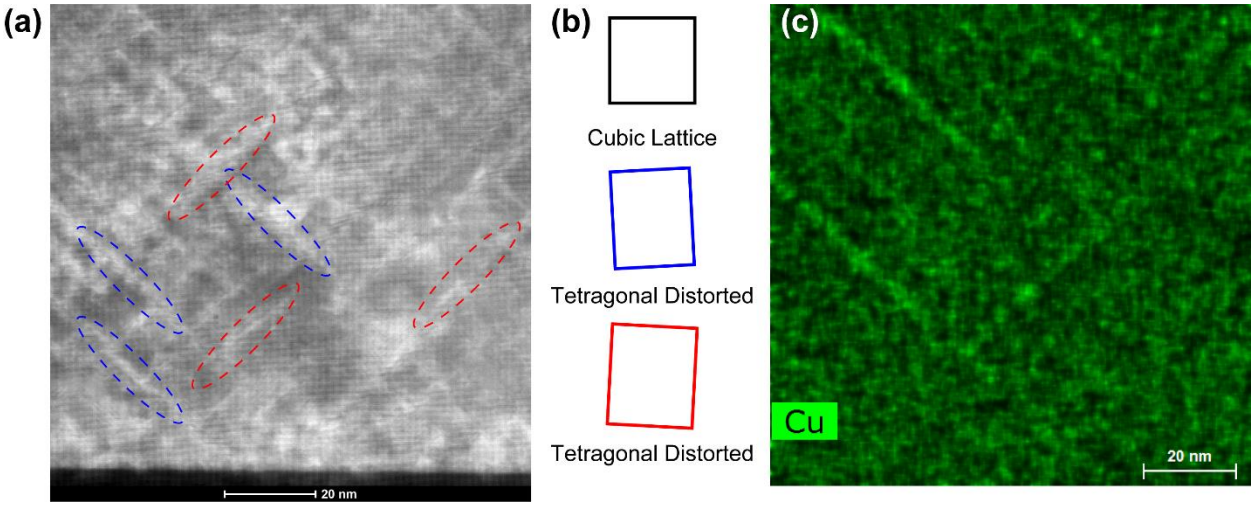

Figure 2. (a) The low angle annular dark field (LAADF) STEM image on the 1Hz & 80nm HEO thin film showing the tweed microstructures. (b) The schematic shows the distortion of the lattice at the tweed microstructures. (c) The energy-dispersive X-ray spectroscopy (EDX) elemental mapping for Cu ions shows the increased concentration locally at the tweed microstructure.

References:

[1] C.M. Rost, E. Sachet, T. Borman, A. Moballegh, E.C. Dickey, D. Hou, J.L. Jones, S. Curtarolo, J.P. Maria, Entropy-stabilized oxides, Nat. Commun. 6 (2015) 1–8. https://doi.org/10.1038/ncomms9485.

[2] A. Sarkar, L. Velasco, D. Wang, Q. Wang, G. Talasila, L. de Biasi, C. Kübel, T. Brezesinski, S.S. Bhattacharya, H. Hahn, B. Breitung, High entropy oxides for reversible energy storage, Nat. Commun. 9 (2018) 1–9. https://doi.org/10.1038/s41467-018-05774-5.

[3] B. Jiang, Y. Yu, J. Cui, X. Liu, L. Xie, J. Liao, Q. Zhang, Y. Huang, S. Ning, B. Jia, B. Zhu, S. Bai, L. Chen, S.J. Pennycook, J. He, High-entropy-stabilized chalcogenides with high thermoelectric performance, Science. 371 (2021) 830–834. https://doi.org/10.1126/science.abe1292.

[4] T. Li, Y. Yao, Z. Huang, P. Xie, Z. Liu, M. Yang, J. Gao, K. Zeng, A.H. Brozena, G. Pastel, M. Jiao, Q. Dong, J. Dai, S. Li, H. Zong, M. Chi, J. Luo, Y. Mo, G. Wang, C. Wang, R. Shahbazian-Yassar, L. Hu, Denary oxide nanoparticles as highly stable catalysts for methane combustion, Nat. Catal. 4 (2021) 62–70. https://doi.org/10.1038/s41929-020-00554-1.

[5] B. Cantor, I.T.H. Chang, P. Knight, A.J.B. Vincent, Microstructural development in equiatomic multicomponent alloys, Mater. Sci. Eng. A. 375–377 (2004) 213–218. https://doi.org/10.1016/j.msea.2003.10.257.

[6] L. Miao, G. Kotsonis, J. Ciston, C. Ophus, J.-P. Maria, N. Alem, Impact of the Synthesis Kinetics of Entropy-stabilized Oxide Thin Films Probed with 4D-STEM and STEM-EELS, Microsc. Microanal. 27 (2021) 352–354. https://doi.org/DOI: 10.1017/S143192762100180X.

[7] G.N. Kotsonis, P.B. Meisenheimer, L. Miao, J. Roth, B. Wang, P. Shafer, R. Engel-Herbert, N. Alem, J.T. Heron, C.M. Rost, J.P. Maria, Property and cation valence engineering in entropy-stabilized oxide thin films, Phys. Rev. Mater. 4 (2020) 100401. https://doi.org/10.1103/PhysRevMaterials.4.100401.

[8] L.M., G.N.K, J.P.M., and N.A acknowledge the support by NSF through the Pennsylvania State University Materials Research Science and Engineering Center DMR 2011839. L.M and N.A. acknowledge the Air Force Office of Scientific Research (AFOSR) program FA9550-18-1-0277 as well as GAME MURI, 10059059-PENN for support. L.M. and N.A. appreciate the support and resources from NSF-MRSEC-sponsored Materials Characterization Lab (MCL) at Penn State.